

resolved with difficulty two γ rays of 0.92 ± 0.03 and 0.96 ± 0.03 Mev.

The γ_2 doublet appears to correlate best with the more precise energy values of Hayward *et al.*¹² if placed in cascade with the 1.45-Mev γ ray. Their 1.83-Mev γ ray corresponds well with the 1.9-Mev γ ray reported here and the 0.94-Mev line appears to be indeed a doublet. Their intensity ratio for the 1.83-Mev line relative to the 0.930-Mev line agrees quite well with that obtained from Y^{92} .

James¹³ recently reported a new 13-hour activity in niobium which he assigned to an isomer of Nb^{92} . This assignment was based primarily on the similarity between the (p, pn) excitation function of this activity and that of the 10-day Nb^{92} . He states that the isomer

emits K x-rays of zirconium and a γ ray whose energy was determined to be 2.35 Mev by a scintillation spectrometer. This γ -ray energy fits well into the level scheme proposed in Fig. 3 and would seem to substantiate the assignment of the 13-hour activity to Nb^{92m} . While one might expect that the 1.42- and 0.47-Mev γ rays would have been also reported as present, they may have been obscured by the 0.93- and 1.83-Mev γ rays of the more abundant 10-day Nb^{92} .

ACKNOWLEDGMENTS

The authors wish to express their thanks to Professor W. C. Parkinson, Professor P. V. C. Hough, and the crew of the University of Michigan cyclotron for their cooperation.

Metastable States of Re^{180} , Ir^{191} , Au^{193} , Pb^{201} , and $Pb^{203}\dagger$ *

VERA KISTIAKOWSKY FISCHER

Radiation Laboratory, University of California, Berkeley, California, and Columbia University, New York, New York

(Received April 25, 1955)

Ten elements of atomic number between 60 and 82 have been bombarded with 31.5-Mev protons and examined for activities with half-lives between 0.5 and 200 seconds. None were observed in Sm, Ho, Tm, Lu, and Ta. Those produced in W, Ir, Pt, Au, and Tl were investigated with scintillation and proportional counters. Isotope assignments were made on the basis of excitation function studies. Observed were Re^{180m} (145 seconds), Ir^{141m} (4.9 seconds), Au^{193m} (3.9 seconds), Au^{195m} (31 seconds), Au^{197m} (7.4 seconds), Pb^{201m} (60 seconds), and Pb^{203m} (6.7 seconds). Decay schemes are proposed and some regularities are discussed.

INTRODUCTION

IN agreement with considerations based on the shell model it has been observed that many isotopes in the region between atomic number 60 and 82 have low-lying metastable states. It has further been pointed out^{1,2} that there is a grouping within this region defined by closed nucleon shells: the density of cases of nuclear isomerism increases sharply at the upper end of the region, there being seven observed cases with $Z=60$ to 72 and twenty-four, with $Z=72$ to 82. In order to determine whether this effect is due solely to insufficient study of the lower end of the region, a search for new cases of isomerism was undertaken.

Ten elements have been bombarded with 31.5-Mev protons and examined for activities with half-life between 0.5 and 200 seconds. These experimentally set limits include the expected half-lives of $M3$ and $E3$ transitions of energy <200 kev, $M4$ and $E4$ transitions of energy >500 kev and energetic beta-decay transitions. Since a number of nuclear reactions are possible

at the maximum bombarding energy, excitation function studies were performed to permit isotopic assignment of the observed activities.

EXPERIMENTAL

I. Bombardment and Counting Arrangement

The ten targets which were bombarded are ^{62}Sm ($>98\%$),³ ^{67}Ho ($>99\%$),³ ^{69}Tm ($>96\%$),³ ^{71}Lu ($>98\%$),³ ^{73}Ta ($>99\%$), ^{74}W ($>99\%$), ^{77}Ir (99.5%), ^{78}Pt ($>99\%$), ^{79}Au ($>99\%$), and ^{81}Tl (99.8%). All of these were in the form of the metal and the numbers in the brackets indicate their elemental purity excluding oxygen contaminations from the formation of oxide coatings.

The bombardments were performed at the University of California Radiation Laboratory linear accelerator. The beam was focused into a spot $\frac{3}{16}$ inch by $\frac{5}{8}$ inch by a strong-focusing magnet consisting of four quadrupole lenses. In addition, to make certain that the beam did not strike the target holder, a collimator was placed immediately before the target position. The energy of the protons from the linear accelerator is 31.5 ± 0.5 Mev; for excitation function studies the desired energies

† This work was sponsored in part by the U. S. Atomic Energy Commission.

* This work was made possible by the Sarah Berliner Fellowship (1953-54) of the American Association of University Women.

¹ M. Goldhaber and R. D. Hill, *Revs. Modern Phys.* **24**, 179 (1952).

² J. W. Mihelich and A. de-Shalit, *Phys. Rev.* **93**, 135 (1954).

³ On loan from Dr. F. H. Spedding, Ames Laboratory, Ames, Iowa.

were obtained by the use of appropriate absorbers placed directly in front of the collimator. The beam current was measured by a gas scintillation beam monitor designed and built by Kitchen,⁴ the output of which was connected to a standard integrating electrometer-recorder. This monitor was placed in the beam path in front of the absorbers and calibrated against a Faraday cup placed in the target position for all absorbers used.

Shielding, consisting of eight inches of paraffin and $\frac{1}{16}$ inch of cadmium, proved sufficient to minimize neutron activation of the NaI(Tl) scintillation crystal used for gamma-ray studies. In addition two inches of lead were used to reduce the external gamma-ray background. During bombardment, the target holder, centered on the beam spot, rested between two vertical rails on a catch. At the end of bombardment the catch was solenoidally withdrawn and the target holder fell, guided by the rails, through a slot in the shielding to a position between a scintillation and a gas counter. Thus the lower limit on the half-lives observable was set by the time of fall, ~ 0.5 second, while the upper limit was set to minimize accelerator idle time.

II. Counters; Electronics

The scintillation counter was of conventional design consisting of a one-inch by $1\frac{1}{2}$ -inch diameter NaI(Tl) crystal and a DuMont 6292 photomultiplier packaged in an aluminum housing and protected by a magnetic shielding and lead shield. Under standard operating conditions, the photopeak of the Cs¹³⁷ 0.66-Mev gamma ray was observed with 8% resolution.

The gas counter was a continuous flow type employing a 90% argon-10% carbon-dioxide mixture. It was operated in the proportional region and used to detect electrons. Energy determinations were made by absorption studies.

A two-pen, three-speed Brush Company recorder was used to record the data. Pulses from the scintillation counter, amplified by a standard University of California Radiation Laboratory nonoverloading linear amplifier, were placed into a scaler connected to one pen of the recorder. The other pen was used to record either the pulses from the gas counter followed by a preamplifier, linear amplifier and scaler, or the pulses from a second output of the scintillation counter linear amplifier followed by an A.I. Model 510 single-channel pulse-height analyzer and a scaler. All the scalers were gated off for the duration of the linear accelerator radio-frequency pulse.

Gamma-ray spectroscopy was performed by using a grey-wedge pulse-height analyzer which has been described previously.⁵

⁴ S. W. Kitchen, Rev. Sci. Instr. **26**, 234 (1955).

⁵ Vera Kistiakowsky Fischer, Phys. Rev. **96**, 1549 (1954).

III. Method

The control used to end bombardment by shutting a flip gate or dephasing the Van de Graaff and linear accelerator, simultaneously started the recorder chart drive. Thus the starting points of the recorder traces correspond to end of bombardment. At the same time the target was dropped. The decay after each bombardment was followed until the counting rate due to longer-lived activities and external background became constant enough to permit resolution of the decay curves.

The spectra of gamma-ray energies were studied with the grey-wedge pulse-height analyzer by exposing a given negative for a time interval after bombardment in which pulses from the desired activity were predominant. This was repeated until sufficient pulses for an intelligible spectrum were accumulated. The general method has been previously described.⁵ Energy calibrations were made at intervals throughout each series of bombardments. The relative intensities of observed gamma rays were determined with the single-channel pulse-height analyzer. Decay curves simultaneously recorded on the differential and integral counting rates were resolved and the components were extrapolated to the time at end of bombardment. The ratio of these extrapolated counting rates were plotted as a function of pulse-height analyzer setting. The heights of the photopeaks corrected by empirical counting efficiency factors and calculated absorption corrections gave the relative intensities. The *K* x-ray values were corrected for the Auger effect.⁶

Absorption curve determinations were made of the electron energies associated with each activity. Ratios of gas counter to scintillation counter counting rates at end of bombardment were plotted as a function of absorber thickness, and these curves were resolved. Electron to gamma-ray intensity ratios were corrected by the factors mentioned for gamma rays, by electron absorption corrections, and for the geometries of the two counters.

Relative cross sections for the excitation functions were calculated from the counting rates of components of the resolved scintillation counter decay curves extrapolated to the end of bombardment. These were corrected as previously discussed and also by a saturation factor calculated from the length of bombardment. Absolute cross-section values were obtained by applying additional corrections for geometry, isotopic abundance, and branching ratio and conversion considerations.

IV. Results

Bombardment of Sm, Ho, Lu, Tm, and Ta yielded only very weak traces of short-lived activities. The amounts corresponded to cross sections of at least a factor of 10^5 smaller than the compound nucleus

⁶ H. S. W. Massey and E. H. S. Burhop, Proc. Roy. Soc. (London) **153**, 661 (1935-36).

TABLE I. Summary of results.

Target Z	Element	Observed half-life (seconds)	Gamma-ray energies (keV)		Electron energies (MeV)	Assign- ment
74	W	145±4[38]	880±40	510±20 106±10	1.1±0.1 <0.3	Re ^{180m}
77	Ir	4.91±0.14[55]	135±10	65±10	<0.3	Ir ^{191m}
		3.88±0.25[69]	255±20	70±10	<0.3	Au ^{193m}
78	Pt	30.6±0.19[65]	260±20	70±10	<0.3	Au ^{195m}
		7.23±0.28[40]	270±20	130±10 70±10	<0.3	Au ^{197m}
79	Au	30.0±1.74[24]	260±20	70±10	<0.3	Au ^{195m}
		6.73±0.44[68]	860±40	75±10	<1.0	Pb ^{203m}
81	Tl	60.1±4.4[42]	650±30	75±10	<1.0	Pb ^{201m}

formation cross sections for the given target and energy. The characteristics of the activities in so far as they could be determined indicated that they probably arose from oxygen and other low-*Z* elements.

Table I summarizes the results with the other five targets. The half-lives quoted represent averages of those determinations which satisfied certain statistical criteria; the errors are their standard deviations. The number of determinations represented by each value is given in the brackets. No quantitative attempt to estimate systematic errors was made. However, the internal consistency between different runs under varying conditions indicates that they are not more than a few percent. In the fourth column, listing the observed gamma-ray energies, the 65–75-keV radiations observed in all cases are probably *K* x-rays. The errors given are estimated experimental errors. The electron energies as measured by the absorption studies are given in the fifth column. The only case where a good end-point determination was possible was wolfram. In all other cases only upper limits could be set.

The last column of Table I gives the assignments which were made for the observed activities on the basis of the excitation functions given in Figs. 1 and 2. In these the ratio of the experimentally determined cross section to the compound nucleus formation cross section⁷ ($r_0 = 1.3 \times 10^{-15}$ cm) is given as a function of the energy of the bombarding proton in the center of mass system. The uncertainties in energy of the points include the uncertainty concerning the energy of the initial beam and the spread due to target thickness. The uncertainties in cross section include an estimate of the experimental errors but do not include uncertainties in some of the factors involved in calculating the absolute cross sections. A downward pointing arrow indicates that the activity was not observed and only an upper limit could be set.

⁷ J. M. Blatt and V. F. Weisskopf, *Theoretical Nuclear Physics* (John Wiley and Sons, Inc., New York, 1952).

INTERPRETATION OF RESULTS

I. Gold

Two short half-life activities were observed in the gold bombardments. One has a half-life of 7.2 seconds with which are associated 130- and 270-keV gamma rays, *K* x-rays and electrons. This is readily identified with the well-known metastable state of Au¹⁹⁷.⁸ The second activity has a half-life of 30 seconds with which is associated a 260-keV gamma ray, *K* x-rays and electrons. These values agree with those previously found for a metastable state of Au¹⁹⁵.^{9,10} which emits 56.5- and 261.6-keV gamma rays. The 56.5-keV gamma ray is very highly converted and therefore would not have been observed in the present study. The experimentally determined intensity ratios for both isotopes agree very well with the known conversion coefficients. Previously proposed^{8–10} decay schemes for both isomers are given in Fig. 3.

The observed excitation functions are given in Fig. 1(a). Curve A corresponds to the reaction, Au¹⁹⁷(*p, p'*)Au^{197m}, and curve B, to the reaction, Au¹⁹⁷(*p, p2n*)Au^{195m}. The values of the ratio $\sigma_{\text{exp}}/\sigma_c$ are small at all energies, the experimental cross section, σ_{exp} being only a few percent of the compound nucleus formation cross section, σ_c . The total inelastic scattering cross section for 31.5-MeV protons in gold has been shown¹¹ to be 0.29 barn, giving $\sigma_{\text{exp}}/\sigma_c = 0.26$, and the cross section for the reaction Ta¹⁸¹(*p, pn*)Ta¹⁸⁰ with 23.4-MeV protons gives $\sigma_{\text{exp}}/\sigma_c = 0.1$.¹² Both of these values represent upper limits for the formation probability of any excited state in the product nucleus and thus a $\sigma_{\text{exp}}/\sigma_c$ of a few percent would be expected for such a reaction. The (*p, p'*) curve, curve A, rises with increasing bombardment energy to 15 MeV, the height of the potential barrier in gold. Then it drops off due to the increasing probability that the residual

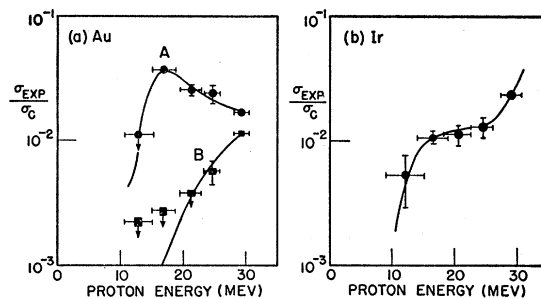


Fig. 1. Excitation functions. (a) Activities produced by bombardment of gold with protons; A: 7.4-second half-life; B: 30-second half-life. (b) 4.9-second half-life activity produced by bombardment of iridium with protons.

⁸ J. W. Mihelich and A. de-Shalit, *Phys. Rev.* **91**, 781 (1953).

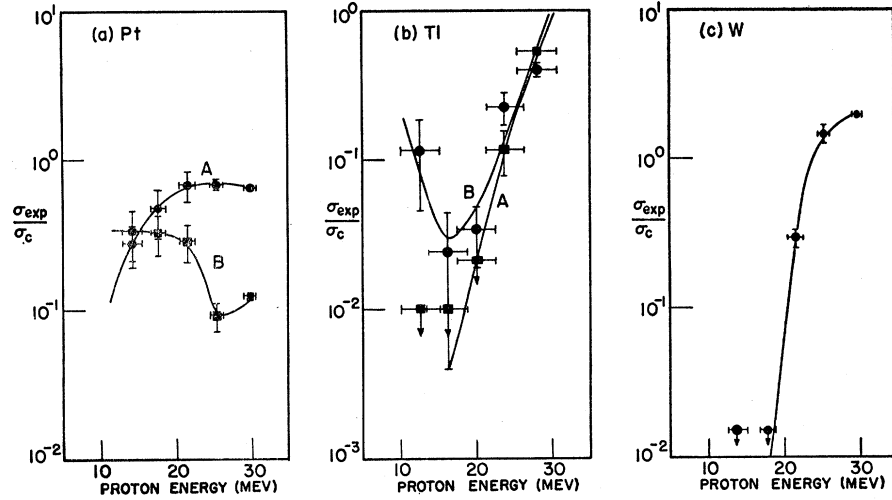
⁹ Huber, Halter, Joly, Maeder, and Brunner, *Helv. Phys. Acta* **26**, 591 (1953).

¹⁰ Grillon, Gopalakrishnan, de-Shalit, and Mihelich, *Phys. Rev.* **93**, 124 (1954).

¹¹ R. M. Eisberg and G. Igo, *Phys. Rev.* **93**, 1039 (1954).

¹² Cohen, Newman, Charpie, and Handley, *Phys. Rev.* **93**, 1039 (1954).

FIG. 2. Excitation functions. (a) Activities produced by bombardment of platinum with protons; A: 3.9-second half-life; B: 31-second half-life. (b) Activities produced by bombardment of thallium with protons; A: 60-second half-life; B: 6.7-second half-life. (c) 145-second half-life activity produced by bombardment of wolfram with protons.



nucleus will still have sufficient excitation energy to emit another particle. The $(p, p2n)$ curve, curve A, rises sharply above 20 Mev which is approximately the threshold for emission of three particles from the compound nucleus.

II. Platinum

Of the two activities observed after the bombardment of platinum, the one with 30.6-second half-life can be immediately assigned to Au^{195m} on the basis of half-life, gamma-ray energy and K conversion coefficient. Furthermore, the excitation function for this activity, Fig. 2(a) curve B, is what would be expected from the sum of the reactions $Pt^{195}(p, n)Au^{195m}$, $Pt^{196}(p, 2n)Au^{195m}$, and $Pt^{198}(p, 4n)Au^{195m}$. Both curves in this figure have not been corrected for isotopic abundance and σ_{exp}/σ_c would be approximately one at lower energies if this correction were made. In this atomic number region such a value indicates that the decay mode of the compound nucleus leading to the isotope in question does not involve charged particle emission. The shape, first constant and then falling off after 20 Mev, indicates that (p, n) and $(p, 2n)$ but not $(p, 3n)$ contribute, while the upward turn at 30 Mev can be explained by a $(p, 4n)$ contribution.

Curve A is the excitation function for the production of the 3.88 second activity. On the basis of similar arguments it is assigned to Au^{193m} produced by the reactions $Pt^{194}(p, 2n)Au^{193m}$, $Pt^{195}(p, 3n)Au^{193m}$, and $Pt^{196}(p, 4n)Au^{193m}$. The initial rise in the curve indicates the absence of (p, n) contribution. This isomer was observed to emit a 255-keV gamma ray with $\alpha_K=0.4\pm 0.1$ and $K/L\sim 2$. Comparing these numbers with the theoretical α_K values given by Rose *et al.*¹³ and the empirical K/L curves given by Goldhaber and Sunyar,¹⁴ the transition is found to be $M1$ with possible $E2$ admixture.

¹³ Rose, Goertzel, Spinrad, Harr, and Strong, Phys. Rev. 84, 1056 (1951).

¹⁴ M. Goldhaber and A. W. Sunyar, Phys. Rev. 83, 906 (1951).

Thus the multipole order of the gamma ray is definitely too low to account for the half-life and some other transition must be rate-determining.

Grillon *et al.*¹⁰ have discovered a metastable state in Au^{198} following the electron capture decay of Hg^{198m} whose half-life they were not able to determine. They observed conversion electrons corresponding to 31.9-keV ($E3$), 257.9-keV ($M1$) and 291-keV (weak) gamma rays. The 257.9-keV gamma ray and the 260-keV gamma ray observed in the present study are presumably identical. The other two would not have been observed. Thus the decay scheme given by Grillon *et al.*,¹⁰ Fig. 3(c), is assigned to the 3.88-second Au^{193m} .

III. Iridium

Figure 1(b) shows the excitation function obtained for the production of the 4.91-second half-life activity in iridium. The σ_{exp}/σ_c values are of the order of magnitude expected for reactions involving emission of charged particles from the compound nucleus. The shape of the curve indicates contributions from (p, p') and $(p, p2n)$ but not (p, pn) . Therefore this activity is assigned to a metastable state in Ir^{191} produced by $Ir^{191}(p, p')Ir^{191m}$ and $Ir^{193}(p, p2n)Ir^{191m}$. Assuming all K

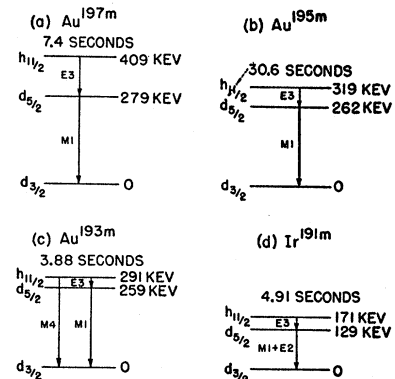


FIG. 3. Decay schemes.

- (a) Au^{197m} ,
- (b) Au^{195m} ,
- (c) Au^{193m} ,
- (d) Ir^{191m} .

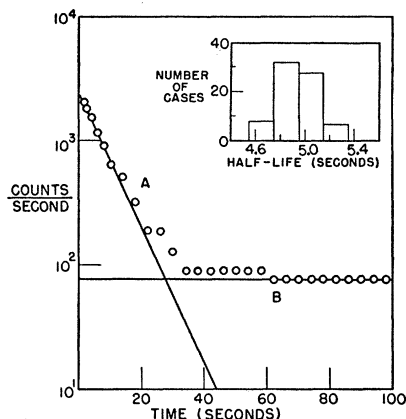


FIG. 4. Typical decay curve for Ir^{191m} . The points are experimental and are resolved into two components, (A) 4.9-second half-life, (B) background. The insert gives the distribution of values determined for the half-life.

x-rays and electrons to arise from the conversion of the observed 135-keV gamma ray it is found that $\alpha_K = 2.7 \pm 0.5$ and $K/L \sim 0.08$.

A 129.1-keV gamma ray going to the ground state of Ir^{191} has been observed both from the decay of Os^{191} ¹⁵⁻¹⁹ and of Pt^{191} .^{10,20} The gamma ray has $\alpha_K = 2.1$ and $K/L = 2.2$ and thus the transition is a mixture of $M1$ and $E2$. Identifying this with the observed gamma ray, the discrepancy in K/L ratios would be explained by a highly L -converted gamma ray corresponding to the rate determining transition. A reasonable choice for this would be the 41.7-keV gamma ray observed preceding the 129.1-keV gamma ray in the decay of Os^{191} .¹⁵⁻¹⁹ Its $L_{II}:L_{III}$ ratio is compatible with assignment to an $E3$ transition.

In two recent papers, experiments are reported in which half-lives of 6.8 ± 1.0 seconds²¹ and 5.6 ± 0.4 seconds²² have been observed for a metastable state of Ir^{191} which emits a 130-keV gamma ray. In one of them, Mihelich, McKeown, and Goldhaber²¹ give a very convincing argument for the same decay scheme suggested here and illustrated in Fig. 3(d). Figure 4 shows a typical decay curve and, in the insert, the distribution of values obtained for the half-life in this experiment.

IV. Thallium

Figure 2(b), curve A, shows the excitation function obtained for the 60-second activity produced by bombardment of thallium. It has both the magnitude and

¹⁵ J. B. Swan and R. D. Hill, Phys. Rev. **88**, 831 (1952).

¹⁶ E. Kondaiah, Arkiv Fysik **3**, 47 (1952).

¹⁷ S. A. E. Johansson, Arkiv Fysik **3**, 533 (1952).

¹⁸ R. D. Hill and J. W. Mihelich, Phys. Rev. **89**, 323 (1953).

¹⁹ F. F. McGowan, Phys. Rev. **93**, 163 (1954).

²⁰ Cork, Brice, Schmid, Hickman, and Nine, Phys. Rev. **94**, 1218 (1954).

²¹ Mihelich, McKeown, and Goldhaber, Phys. Rev. **96**, 1450 (1954).

²² R. A. Naumann and J. B. Gerhart, Phys. Rev. **96**, 1452 (1954).

shape expected for a $(p,3n)$ reaction. Curve B, that for the 6.7-second activity observed, has a shape resembling a (p,n) curve at low energies and $(p,3n)$ at high, with no $(p,2n)$ component. Thus the 60-second activity has been assigned to a metastable state of Pb^{201} from $\text{Tl}^{203}(p,3n)\text{Pb}^{201m}$ and the 6.7-second activity to a metastable state of Pb^{203} from $\text{Tl}^{203}(p,n)\text{Pb}^{203m}$ and $\text{Tl}^{205}(p,3n)\text{Pb}^{203m}$. Hopkins²³ also bombarded thallium with protons and observed 50-second and 5.6-second half-life activities which he identified as Pb^{201m} from $\text{Tl}^{203}(p,3n)\text{Pb}^{201m}$ and Pb^{202m} from $\text{Tl}^{203}(p,2n)\text{Pb}^{202m}$. The second assignment was based on observing the activity with a bombarding energy of 22 Mev but not with 17 Mev.²⁴ This was not the case in the present work, as seen in Fig. 5 which shows a typical decay curve obtained with bombarding energy ≤ 15.2 Mev. Figure 6 shows a typical decay curve from maximum energy bombardment, with an insert which gives the observed distribution of half-life values. An explanation for the discrepancy between the 6.73-second half-life observed in this experiment and the 5.6-second value previously obtained has not been found.

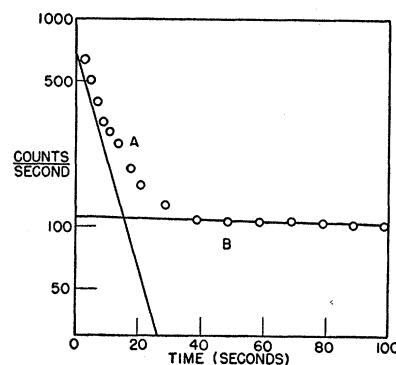


FIG. 5. Typical decay curve for Pb^{203m} produced by bombardment of thallium with protons of energy ≤ 15.2 Mev. The points are experimental and are resolved into two components: A, 6.7-second half-life; B, background.

It was found in the present study that a 0.86-MeV gamma ray with $\alpha_K = 0.13 \pm 0.06$ is emitted by Pb^{203m} . This is in best agreement with the theoretical value of an $M4$ transition.¹³ The ground state of Pb^{203} has been found to be $f_{5/2}$ from its electron capture decay scheme.²⁵ This and the shell model suggest that the state is $i_{13/2}$ as illustrated in Fig. 7(a). Using the semiempirical formula given by Goldhaber and Sunyar¹⁴ for the mean life, τ_γ , of an $M4$ transition:

$$\tau_\gamma = 1 \times 10^4 (2i+1) / A^2 E^9,$$

where i is the spin of the initial state and E , the energy of the transition in Mev, an expected half-life of 7.2 seconds is calculated for Pb^{203m} , in excellent agreement with the experimental value.

In the present work, Pb^{201m} was observed to decay with a 60.1-second half-life emitting a 0.65-MeV gamma with $\alpha_K = 0.75 \pm 0.25$. This is in best agreement with the theoretical value for an $M4$ transition.¹³ Hopkins²³

²³ N. J. Hopkins, Phys. Rev. **88**, 680 (1952).

²⁴ N. J. Hopkins (private communication, 1955).

²⁵ J. Varma, Phys. Rev. **94**, 1688 (1954).

reported a 56-second half-life and 0.67-, 0.42-, and 0.25-Mev gamma rays. More recently his work has been repeated and the two lower-energy gamma rays were not observed.²⁴ The half-life calculated for this transition using the Goldhaber-Sunyar equation¹⁴ is 61 seconds, again in good agreement with the experimental value. Thus the decay scheme shown in Fig. 7(b) is proposed for Pb^{201m} in analogy to that for Pb^{203m}.

V. Wolfram

Figure 2(c) shows the excitation function obtained for the 145-second activity produced in wolfram. The order of magnitude of the maximum value and the shape of the curve assign the activity to the product of a (*p*,3*n*) reaction alone. Thus it must be Re¹⁸⁰ from W¹⁸²(*p*,3*n*)Re¹⁸⁰. The contribution from W¹⁸⁰(*p*,*n*)Re¹⁸⁰ is not seen because of the 0.135% abundance of W¹⁸⁰.

Gamma rays with energies of 880 kev, 510 kev, and

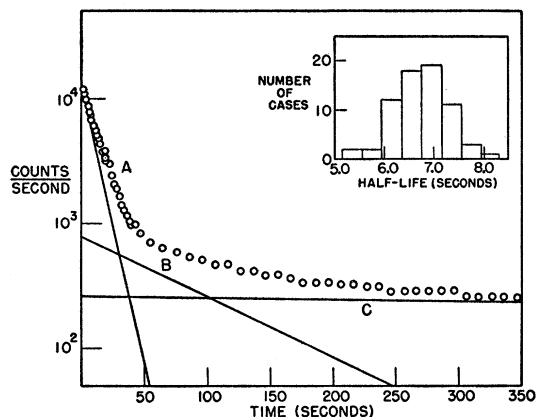


FIG. 6. Typical decay curve for Pb^{201m} and Pb^{203m}. The points are experimental and are resolved into three components: A, 6.7-second half-life; B, 60-second half-life; C, background. The insert gives the distribution of values determined for the shorter half-life.

106 kev; *K* x-rays; electrons and a beta-particle group of maximum energy 1.1 Mev were observed from the decay of this isotope. It is calculated from the semi-empirical mass equation²⁶ that the ground state of Re¹⁸⁰ is unstable by 2.8 Mev with respect to the ground of W¹⁸⁰, suggesting that the 1.1-Mev beta particle is a positron. That this is the case and that the 0.51-Mev gamma ray is annihilation radiation is confirmed by the ratio of their intensities, $N_{\beta, 1.1 \text{ Mev}}/N_{\gamma, 0.51 \text{ Mev}} = 0.7 \pm 0.4$. The theoretical ratio of *K* electron capture to positron emission is found to be $f_K/f_+ = 50$ from the curves of Feenberg and Trigg²⁷ and it is calculated that $\log ft_{\beta^+, K} = 4.0$. A correction for *L* electron capture²⁸ raises this to $\log ft_{\beta^+, K} = 4.1$.

The ratio of the intensity of the 1.1-Mev positron-

²⁶ N. Metropolis and G. Reitwiesner, "Table of Atomic Masses," Atomic Energy Commission Report NP-180, 1950 (unpublished).
²⁷ E. Feenberg and G. Trigg, Revs. Modern Phys. **22**, 399 (1950).
²⁸ M. E. Rose and J. L. Jackson, Phys. Rev. **76**, 1540 (1949).

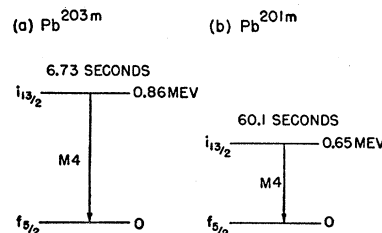


FIG. 7. Decay schemes. (a) Pb^{203m} (b) Pb^{201m}

electron capture decay branch to that of the 0.88-Mev gamma ray is $[(f_+ + f_K)/f_+]N_{\beta, 1.1 \text{ Mev}}/N_{\gamma, 0.88 \text{ Mev}} = 10 \pm 4$. Thus these transitions are not in sequence and the 0.88-Mev gamma ray probably follows an electron capture decay to an excited level in W¹⁸⁰. If one assumes that the energy of this transition is $(E_{\beta^+} + 1.0) - E_{\gamma} = 1.2$ Mev, it is found that $\log ft = 4.6$. When $\log ft_{\beta^+, K}$ is corrected for this branching, it is still 4.1. This suggests that there must be a third competing decay mode and an obvious choice, in view of the radiations observed, is that electron capture and positron decays proceed from a metastable state of Re¹⁸⁰. The 106-kev gamma ray is possibly emitted in this suggested isomeric transition. However, Brown *et al.*²⁹ observed a level of W¹⁸⁰ 102 kev above the ground state. By analogy to Hf¹⁸⁰ and all other stable even-*A* wolfram isotopes which have 2+ rotational states at about 100 kev,³⁰ this is probably an *E2* transition. The observed 106-kev gamma ray may also be partially or completely due to this transition and a number of decay schemes are possible as indicated in Fig. 8.

CONCLUDING REMARKS

Of the ten targets studied, only those at the upper end of the atomic number region gave observable activities. In view of the limitations of the experiment, this is not conclusive but it does substantiate the previously mentioned effect. There are now seven known cases of isomerism between *Z*=60 and 72, and twenty-seven between *Z*=72 and 82. Goldhaber and Hill¹ and Mihelich and de-Shalit² have suggested that the absence of odd-proton isomers in the lower region can be

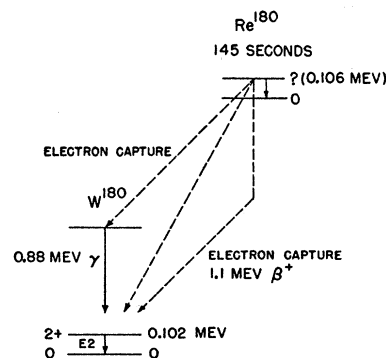


FIG. 8. Decay scheme proposed for Re^{180m}.

²⁹ Brown, Bendel, Shore, and Becker, Phys. Rev. **84**, 292 (1951).
³⁰ N. P. Heydenburg and G. M. Temmer, Phys. Rev. **93**, 906 (1952).

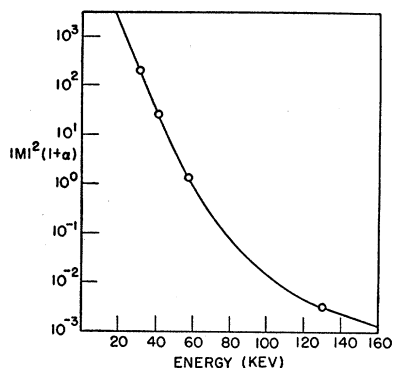


FIG. 9. $|M|^2(1+\alpha)$ as a function of transition energy for $E3$ transitions between $h_{11/2}$ and $d_{5/2}$ levels in odd-neutron Au and Ir isotopes.

explained by the destruction of the metastability of the expected single-particle levels through the intervention of low-lying levels of the coupled system.

Mihelich and de-Shalit² have pointed out that the transition matrix elements, $|M|^2$, for the $M4$ transitions between $i_{13/2}$ and $f_{5/2}$ states in odd-neutron Pb, Hg, and Pt isotopes show a dependence on nucleon number. $|M|^2$ is defined as the ratio of the mean life for the transition calculated as in Blatt and Weisskopf⁷ to the experimental value corrected for conversion. Table II

TABLE II. Values of $|M|^2$ for $M4$ transitions.

N	115	117	119	120	123	125
Pb			1.02	1.18		1.54
Hg	0.88	1.02	1.00			
Pt		0.77	0.98			

combines the values for Pb^{201m} and Pb^{203m} observed in the present study with those previously given.² It again emphasizes that $|M|^2$ increases as the nucleon numbers of the isomers approach closed shells. The observation however, that this increase is less than a factor of two accounts for the success of Goldhaber and Sunyar¹⁴ in fitting an expression to the observed half-lives without considering closed shell effects.

The $E3$ transitions between $h_{11/2}$ and $d_{5/2}$ levels in the odd-neutron Au and Ir isomers might be expected to show similar behavior. Since accurate values for the conversion coefficients of low-energy $E3$ gamma rays are not yet available, nothing can be said about $|M|^2 \cdot |M|^2(1+\alpha)$, where α is the total conversion coefficient, is plotted against transition energy in Fig. 9 and is seen to be a smooth and rapidly decreasing

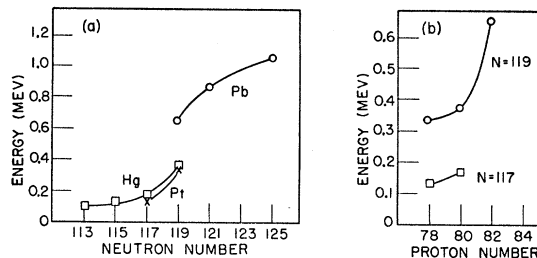


FIG. 10. Energy separation of $i_{13/2}$ and $f_{5/2}$ levels in odd- A Pt, Hg, and Pb isotopes (a) as a function of neutron number, (b) as a function of proton number.

function. If one assumes that $|M|^2$ does not vary by large factors as is the case in the $M4$ transitions discussed above, then the curve is essentially the energy dependence of $(1+\alpha)$.

It has been shown² that the energy separation of the $i_{13/2}$, $f_{5/2}$, and $p_{1/2}$ levels changes smoothly with neutron number in odd-neutron Pt and Hg isotopes. In Fig. 10(a), the energy separation of the $i_{13/2}$ and $f_{5/2}$ levels in Pb, Pt, and Hg isotopes is plotted against neutron number. The values for Pb^{201m} and Pb^{203m} were those observed in this experiment while those for the other isomers were taken from the article by Mihelich and de-Shalit.² Figure 10(b) shows the energy separation plotted against proton number for neutron number 119 and 117. In both cases the level separation is seen to increase smoothly as expected as the nucleon number approaches a closed shell value.

ACKNOWLEDGMENTS

The support of this work by the Sarah Berliner Fellowship (1953-54) of the American Association of University Women is acknowledged with great pleasure. Professor L. W. Alvarez is gratefully thanked for his encouragement and sponsorship of this research. Many thanks are also due to Mr. R. Watt and all the members of the linear accelerator crew for their patient assistance and to the members of Mr. Farnsworth's group for their help in assembling and maintaining the electronics. The author is much indebted to Dr. F. H. Spedding for loaning her the rare earth samples and to Professor J. M. Miller for making possible the completion of the work at Columbia University. Several helpful discussions with Dr. L. J. Lidofsky are gratefully acknowledged.